

# High Reliability Technology of the Weld Zone of High-Frequency Electric Resistance Welding Linepipes<sup>†</sup>

OKABE Takatoshi<sup>\*1</sup> IIZUKA Yukinori<sup>\*2</sup> IGI Satoshi<sup>\*3</sup>

## Abstract:

High-frequency electric resistance welding (HFW) steel pipe is used in high-grade pipelines and energy field. To address the significant need for weld seam reliability, we have developed welding technology, high sensitivity ultrasonic inspection technology, and quality assessment technology for HFW pipe. HFW phenomena were visualised dynamically using a high-speed video camera. Furthermore, an HFW numerical analysis model was constructed to develop optimization technology of HFW conditions and the homogeneous heating technology of the weld zone. The Charpy fracture transition temperature of the weld metal of the developed steel pipe was  $-90^{\circ}\text{C}$  showing the high absorbed energy value at cryogenic temperature. Furthermore, real-time continuous detection technology of the oxide of the weld zone was developed by a point converging tandem beam ultrasonic inspection method. This technology achieved high sensitivity 10 times or more than that of the conventional method. It was possible to detect the oxide which decreases the toughness of weld metal. It was successfully achieved to guarantee the stabilized quality covering full length in the weld zone. By the evaluation test using a full-body pipe, it became clear that the developed steel pipe does not cause the brittle fracture at the low temperature environment of  $-45^{\circ}\text{C}$ .

## 1. Introduction

High-frequency electric resistance welded (HFW) steel pipes have many excellent properties, such as a clean skin surface and accuracy of shape dimensions. The material design, manufacturing processes, and qual-

ity control technology used in the HFW steel pipe production have been significantly advanced by research and technological developments throughout the years. As a result, these pipes are used in wide applications including the energy field, machine structures, and ordinary piping. In recent years, the demand for the HFW pipes with low-temperature toughness has been increased with increasing the cold-region natural gas field. The weld seam toughness of conventional HFW pipes deteriorates in such severe environment<sup>1)</sup>.

In order to improve weld seam toughness, in this research, the welding behavior of HFW was clarified by direct observation of HFW welding phenomena and numerical simulations<sup>2-9)</sup>. The movement behavior of metal oxides in the molten steel and the morphology of the oxides, which affect the mechanical properties of the HFW seam, were clarified. As a result of a development of the homogeneous heating and melting technology, elimination of oxides that from during HFW was promoted, which made the Charpy impact toughness less than  $-90^{\circ}\text{C}$  as a ductile-brittle transition temperature<sup>10,11)</sup>.

In order to guarantee the toughness of the HFW seam over the entire length, a continuous real-time inspection technology for oxides that remains in the weld seam was developed. Online detection during production was achieved by development of an unprecedented ultrasonic flaw detection system, realizing quality inspection of the entire length of the HFW seam<sup>12-15)</sup>.

Furthermore, an evaluation test using a full-body pipe confirmed that the developed pipe secures the low-temperature toughness<sup>11)</sup>. With the innovations mentioned above, HFW steel pipes of JFE Steel have been

<sup>†</sup> Originally published in *JFE GIHO* No. 34 (Aug. 2014), p. 77-83



<sup>\*1</sup> Senior Researcher Manager,  
Tubular Products & Casting Res. Dept.,  
Steel Res. Lab.,  
JFE Steel



<sup>\*2</sup> Dr. Eng.,  
General Manager,  
Instrument and Control Engineering Res. Dept.,  
Steel Res. Lab.,  
JFE Steel



<sup>\*3</sup> Dr. Eng.,  
Senior Researcher General Manager,  
Joining & Strength Res. Dept.,  
Steel Res. Lab.,  
JFE Steel

adopted in extra-low temperature environments, subsea pipelines, and other sever applications.

This paper presents an outline of the HFW technology, a nondestructive evaluation technology, and a quality assessment technology for HFW steel pipes, which are element technologies for the developed pipe.

## 2. Development of HFW Technology

### 2.1 Visualization Technology for HFW Phenomena

HFW steel pipes are manufactured by roll forming. Hot-rolled steel sheets are roll-formed into a circular shape by forming rolls, subsequently, the both edge faces of a hot-rolled sheet are heated up to the melting point by high-frequency electric resistance, then pressurized and bonded (Fig. 1).

First, in order to visualize the welding phenomena and clarify the heating and welding behavior of HFW, HFW pipes were manufactured by laboratory pipe welding equipment with high-frequency induction heating system, and the welding phenomena were observed. Photo 1 shows an image which was captured from immediately above by a high speed camera. The conver-

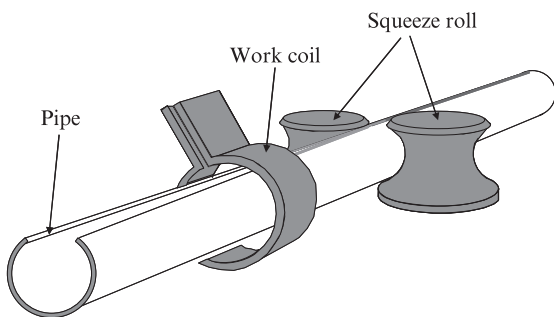


Fig. 1 Production process of high-frequency electric resistance welding (HFW) steel pipe

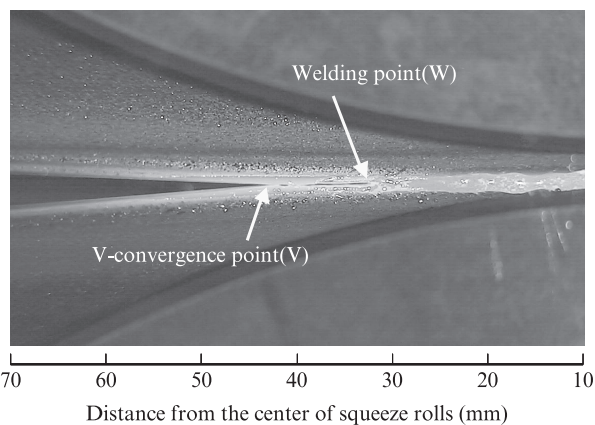


Photo 1 Appearance of welding as captured by high-speed camera

gence point (V) is approximately 42 mm upstream from the center of the squeeze rolls, and the edge faces are completely melted. At the downstream of the welding point (W), excess molten steel rose and piled up on the weld seam due to pressurization by the squeeze rolls and “molten steel pool” was generated. The molten steel solidified about 15 mm upstream from the center of the squeeze rolls.

Visualization of HFW phenomena clarified the fact that melt welding is performed and the molten steel solidifies while pressurizing process. Based on this knowledge, an HFW numerical analysis model was developed concerning the heating behavior before the V point, and the phenomenon of molten steel movement under pressurization after the W point.

### 2.2 Numerical Analysis Technique for HFW Phenomena

Using a numerical analysis technique, a numerical analysis model of the HFW weld seam was developed, and the behavior of HFW was clarified. HFW process can be broadly divided into high-frequency induction resistance welding and high-frequency contact resistance welding<sup>16)</sup>. The HFW phenomena in both welding processes were investigated by preparing respective numerical analysis models for each process.

#### 2.2.1 Numerical analysis technique for high-frequency induction resistance welding

The other numerical analysis model was developed to clarify the temperature distribution of the HFW seam. Figure 2 shows an outline of the numerical analysis model of the HFW seam by high-frequency induction resistance welding. The current density distribution of the pipe was calculated by an electromagnetic analysis, and the temperature distribution of the HFW pipe was then obtained by a heat conduction analysis.

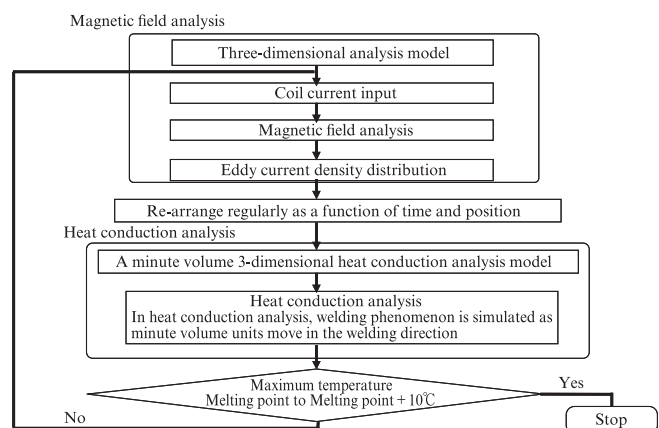


Fig. 2 Analysis flow of electro magnetic and heat conduction finite element analysis (FEA)

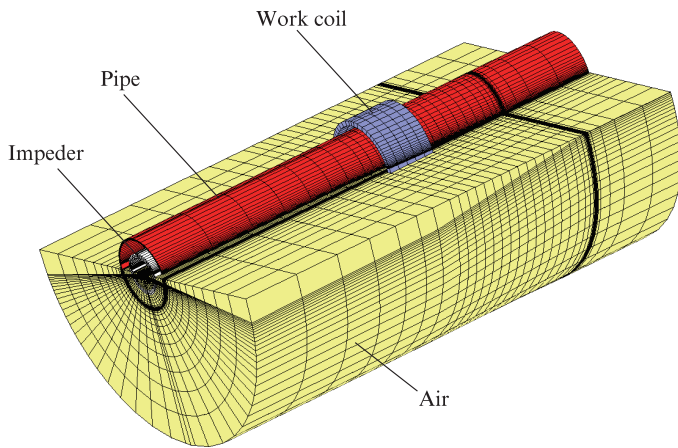


Fig. 3 Meshes of electro magnetic analysis model

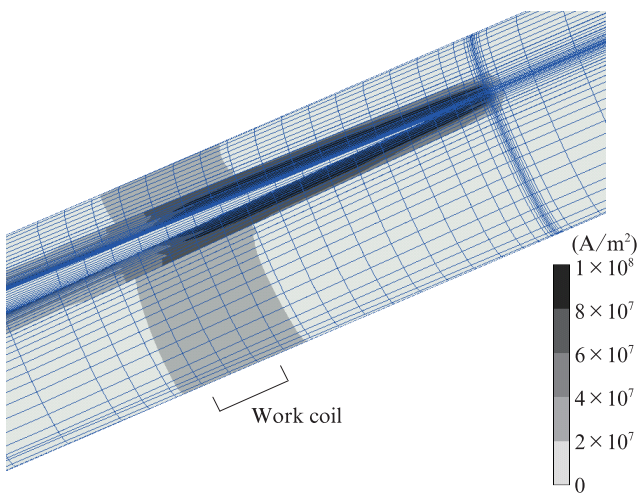


Fig. 4 Contour map of eddy current density

On the assumption that the distribution of the electromagnetic-field in a welding is the same as that in a static state, the eddy current density distribution was calculated by a frequency response analytic law. **Figure 3** shows an overview of the electromagnetic finite element analysis model. The analysis model is a three-dimensional model, and is divided into two parts considering the symmetry of the pipe. Figure 3 shows the full circumference only of the work-coil and the pipe.

**Figure 4** shows an example of the eddy current density distribution calculated with the frequency of 300 kHz and welding speed of 100 m/min. The current density is concentrated immediately below the work-coil and at the edge faces. Under the work-coil position, it is estimated that an eddy current of approximately  $10^7$  A/m<sup>2</sup> flows in the circumferential direction around the full circumference of the pipe. The concentration of the eddy current at the edge started from the work-coil entry side, and reaches approximately  $10^8$  A/m<sup>2</sup> at the work-coil exit side. The eddy current density then increases from the coil exit side to the welding point,

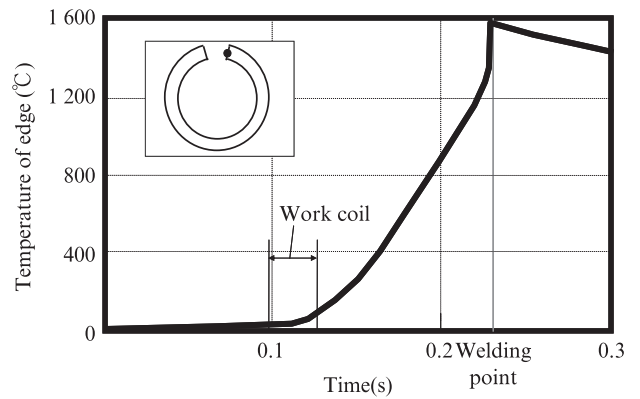


Fig. 5 Relationship of the temperature of edge and time

where it achieves its highest value, and then drops rapidly after passing the welding point, decreasing to  $10^7$  A/m<sup>2</sup> or less at a distance of 0.2 mm from the welding point. A heat conduction analysis was performed based on the results of the electromagnetic analysis in Fig. 4, and the temperature of the edge was analyzed. The results are shown in **Fig. 5**. This analysis revealed that HFW displays the following heating behavior: Heating of the edge begins at passing through the center of the work-coil, and the temperature rises linearly from the end of the work-coil to the entry side of the welding point. The temperature then rises more rapidly from just before the welding point to the welding point itself, after which it gradually decreases.

### 2.2.2 Numerical analysis technique for high-frequency contact resistance welding

**Figure 6** shows an outline of the numerical analysis model of the HFW seam by high-frequency contact resistance welding. In this numerical analysis, an analysis technique combining a two-dimensional model was used. Specifically, a continuous electromagnetic and heat conduction analysis was conducted by subdividing the cross section containing the electrode and the weld-

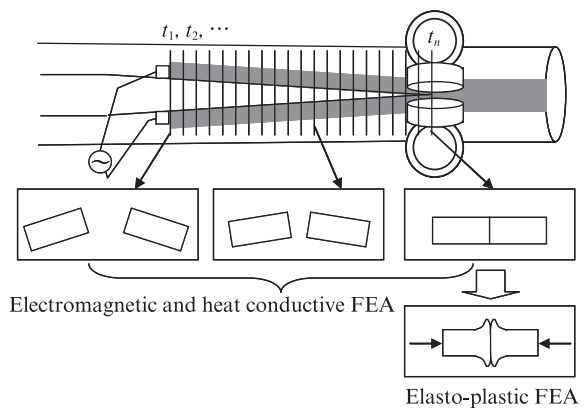


Fig. 6 Overview of finite element analysis (FEA) system for high-frequency electric resistance welding (HFW)

ing point into a large number of two-dimensional models. Initially, a two-dimensional model of a cross section of the electrode is produced, and electromagnetic and heat conduction finite element analysis (FEAs) are executed. Second, an additional two-dimensional model is produced and similar electromagnetic and heat conductive FEAs are executed. The temperature distribution at each position just before the welding point is calculated by repeating this process. At the welding point, elastic plastic FEA starts. The mesh of both pipes is transferred horizontally while keeping the temperature distribution at the welding point, and the deformation behavior of the welding portion is analyzed.

In the analysis, an elastic plastic structural analysis method by the transient response analysis was used. An HFW simulation system combining electromagnetic, heat conductive, and elastic plastic FEA methods was developed, and the deformation behavior of the HFW seam was clarified. The relative permeability, specific heat, electric resistance, enthalpy, thermal conductivity, stress, and the Young's modulus of the pipe are used as a function of temperature.

The effects of the forming conditions and welding conditions on HFW phenomena were investigated by using this analysis method. As examples, **Figs. 7** and **8** show the effect of welding speed on the equivalent plastic strain distribution contour maps and stress distribution contour maps after pressurization of the welding portion, respectively. From Fig. 7, as the welding speed increased, the shape of the excess metal on the inside and outside changed from a wide, gently-sloping shape to a narrow, steep one. At 0.1 m/s, strain was widely distributed in the pipe circumferential direction, and the maximum strain at the butting faces was 1.2. As the welding speed increased, strain became narrow in the circumferential direction, changing to a local distribution, and accompanying this, the strain at the butting faces increased to a maximum of 1.8. According to Fig. 8, the stress in near the welding edge is low at low welding speeds, and as the welding speed increases, the stress in near the welding edge also increases remarkably. When the welding speed is low, the heating width is wide and the entire weld zone is heated to a high temperature. As a result, it can be inferred that the deformation resistance of the weld zone decreases, the entire weld zone can be pressurized at low stress, and the strain of the butting faces decreases. On the contrary, the welding speed increases, the heating width becomes narrow, the amount of melting decreases, and consequently, the deformation resistance in the area near the welding edge increases; under this condition, it can be assumed large strain is generated locally in the welding edge. Furthermore, the strain rate of the weld zone also increases at higher welding speeds. As a result of these

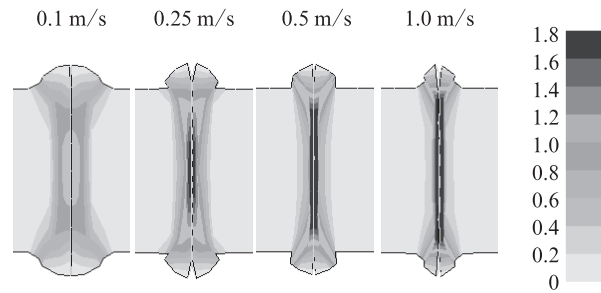


Fig. 7 Effect of welding speed on strain distribution

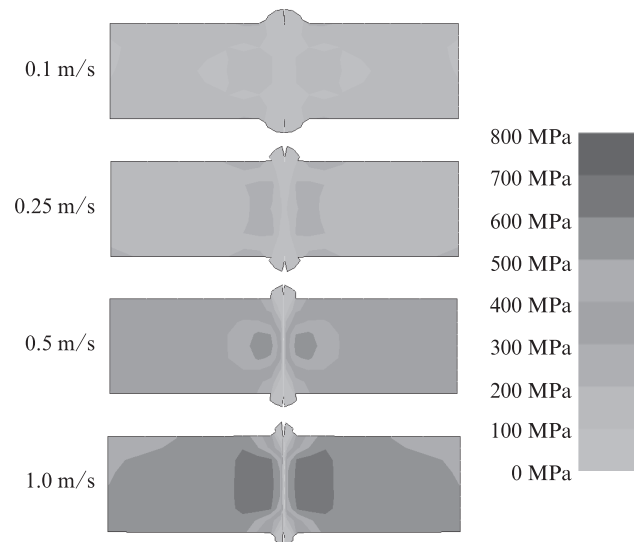


Fig. 8 Effect of welding speed on stress distribution

effects, it is estimated that molten steel at the edge and oxides in the molten steel are pushed out more easily to the excess metal. Thus, it was estimated that increasing the welding speed is effective from the viewpoint of prevention of metal oxides.

### 2.2.3 Behavior of molten metal and oxides in HFW

A numerical analysis system was developed in order to clarify the movement of oxides in molten metal during pressurization in HFW. Using the temperature distribution of the weld zone obtained by the procedure in Fig. 6 as an initial value, an analysis combining the heat conductive and plastic flow analyses by the two-dimensional model was executed. As an initial condition, assuming an oxide film with a uniform thickness of 100  $\mu\text{m}$  exists on the surface of the molten steel at the welding edge, **Fig. 9** shows the results of an analysis of the oxide movement during the pressurization process. As pressure increases, the molten steel moves upward, and the oxide film on the edge face also moves upward, beginning just after pressurization. After 0.06 s, most oxides move to the excess metal, and with increasing time, those in the metal are stirred and rise upward.

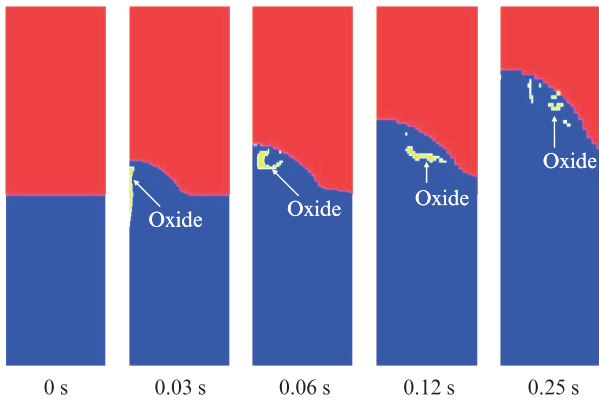


Fig. 9 Oxide distribution during pressurisation from welding rolls

Assuming the initial oxide content is 1, the oxide content in the excess metal was about 0.98. Thus, this analysis revealed that a large majority of the oxides that exist at the welding edge faces are pushed out to the excess metal. Furthermore, the new knowledge that elimination of oxides becomes remarkably easier as a result of homogenous heating of the edge through the entire wall-thickness was obtained.

### 2.3 Development of HFW Technology

Based on the knowledge obtained by direct observation and numerical analysis of HFW phenomena, HFW conditions were optimized and a technology for homogeneous heating of the weld zone was developed. Because the metal oxides that generate in the weld zone are easily pushed out to the excess metal, the mechanical properties of the HFW seam was improved. **Figure 10** shows the low temperature Charpy toughness of the developed HFW weld seam. The Charpy transition temperature of weld seam of conventional HFW steel pipes was  $-37^{\circ}\text{C}$ , in contrast, that of developed pipes

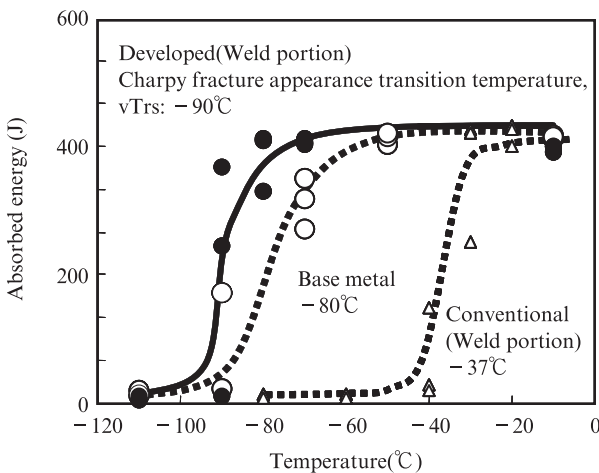


Fig. 10 Low temperature Charpy toughness of high-frequency electric resistance welding (HFW) seam

was  $-90^{\circ}\text{C}$ .

## 3. Development of Quality Assurance Technology for HFW Seam

### 3.1 Outline of Quality Assurance System

Conventionally, quality assurance of HFW pipes was performed by angled-beam ultrasonic testing and destruction testing such as Charpy impact testing. Although entire length inspection is possible by ultrasonic testing, the object of inspections is millimeter-order weld defects and cracks. For evaluation of low temperature toughness, which is influenced by microscopic oxide inclusions, tests of mechanical properties had been used.

Therefore, in order to guarantee the quality of the weld seam over the entire length of the product, the authors developed a nondestructive and online detection technology for microscopic oxide inclusions, which affect low temperature toughness, over the entire length of the weld seam. **Figure 11** shows the overall configuration of the ultrasonic inspection system. This inspection system comprises a phased array ultrasonic inspection system for detection of microscopic oxide inclusions, and a seam detector, position control, and water cooling device, which are equipment for performing online detection immediately after welding. These devices were realized through a process of (1) basic research on detection phenomena, (2) development of detection technology by phased array ultrasonic inspection, and (3) systemization development for online application. The respective stages of this process are described in detail in the following.

### 3.2 Basic Research on Detection Technology for Oxide Inclusions in HFW Weld Seam

In order to assure weld seam quality by detection of oxide inclusions, the state of oxides when they affect

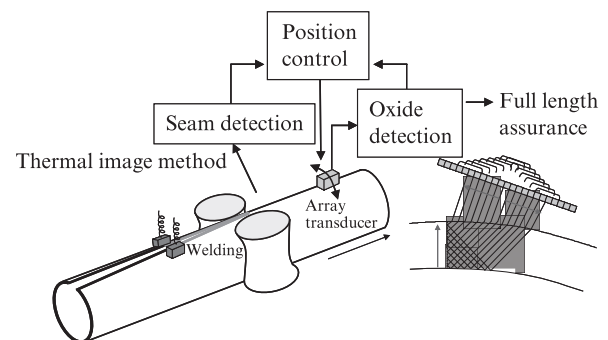


Fig. 11 Outline of quality assurance system of high-frequency electric resistance welding (HFW) steel pipe

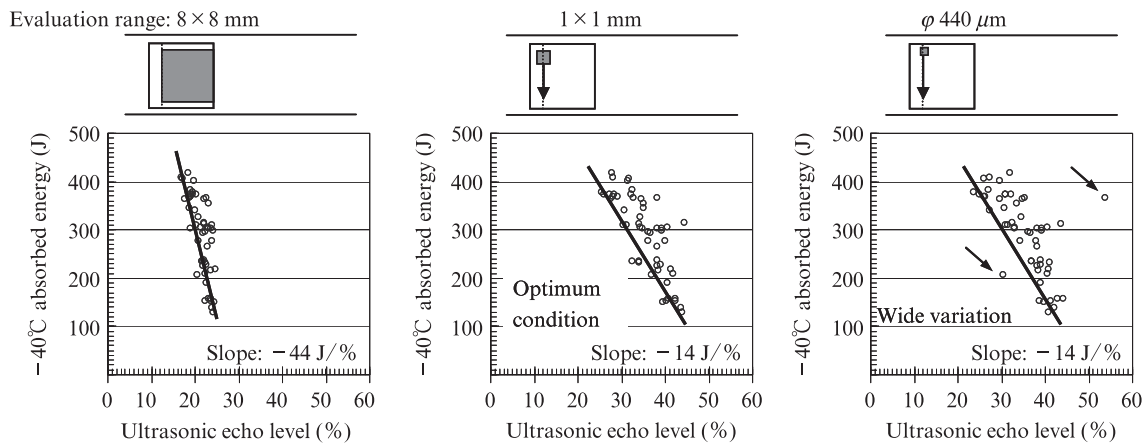


Fig. 12 Optimum high sensitivity ultrasonic inspection condition for quality assurance of high-frequency electric resistance welding (HFW)

low temperature toughness must be detected. Therefore, samples sliced from the weld seam were investigated by using a high sensitivity ultrasonic C-scan test with a focused probe. The results revealed that microscopic oxides with a size of several  $\mu\text{m}$  exist in a scattered distribution in the HFW seam, and areas with a high inclusion density influence low temperature toughness.

Furthermore, absorbed energy in the Charpy impact test was compared with various high sensitivity C scan evaluation ranges. **Figure 12** shows the correlation between the ultrasonic echo levels and absorbed energy with various ultrasonic evaluation ranges. Absorbed energy in the Charpy impact test could be evaluated by the ultrasonic echo amplitude with the optimized highest sensitivity focused beam size, which was about  $1\text{ mm}^2$ . In other words, the distribution of the microscopic oxide inclusions that affect low temperature toughness was successfully evaluated by using the ultrasonic inspection method.

### 3.3 Detection Technology by Phased Array Ultrasonic Inspection

Phased array ultrasonic technology was utilized to perform inspections under the above-mentioned focus condition with the as-manufactured pipe without cutting samples from the weld. A focused beam with a size of  $1\text{ mm}^2$  was realized by transmitting from multiple oscillators with gradually shifted phases. Considering the perpendicularity of the scanning surface, signals were received from the specular reflection direction, as shown in **Fig. 13**, achieving high sensitivity more than 10 times superior to that of the conventional ultrasonic angled beam inspection. In addition, the developed technology makes it possible to scan from the inner surface to the outer surface in the thickness direction of the weld by appropriate control of the transmitting and receiving positions.

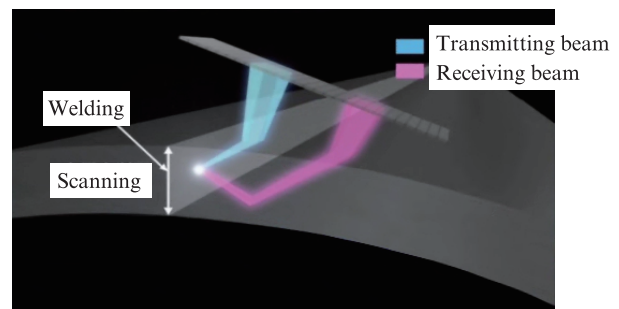


Fig. 13 High sensitivity ultrasonic inspection technology for high-frequency electric resistance welding (HFW) weld seam

### 3.4 Systemization for Online Application and Example of Full-Length Evaluation

As an equipment configuration for continuous scanning of HFW steel pipes in the production process, a precise seam tracking technology was developed to enable the probes to track the weld seam position, which varies in the circumferential direction during pipe production. The weld seam position is measured based on the temperature distribution by the seam tracking system using thermal images, and the seam tracking system aligns the position of the array probes to track the seam, thereby achieving stable online detection. **Figure 14** shows an example of detection when the mechanical properties of the weld zone were degraded intentionally by decreasing the welding heat input to lower than the optimum value. The results demonstrate that the existence of distributed microscopic oxides can be detected with high reliability.

As described above, it has become possible to detect and display the distribution of oxides in real time by complete detection through the thickness and in the longitudinal direction by a nondestructive inspection technology, realizing entire-length quality assurance of the weld seam.

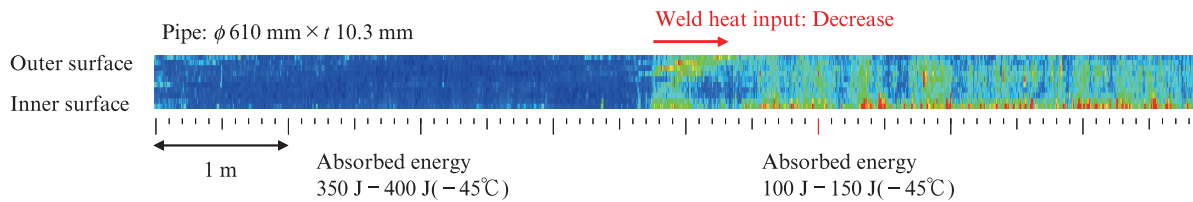


Fig. 14 Quality assessment examination in the high-frequency electric resistance welding (HFW) actual mill

#### 4. Example of Full-Body Pipe Assessment Test

Linepipes are required to demonstrate their functions safely over a long period of time from pipe laying until actual service. Therefore, characteristic data on the deformation and rupture behavior of actual full-scale pipes are extremely important. These data support adoption of the optimum product for the service environment and operating conditions and securing its integrity. To confirm the fracture behavior of the developed steel pipe in low temperature environments, low temperature burst tests with a notched seam were conducted at  $-20^{\circ}\text{C}$  and  $-45^{\circ}\text{C}$  by using full-body pipes. An artificial defect was introduced in the HFW seam. **Photo 2** and **Fig. 15** show examples of the results. The two lines in Fig. 15 show

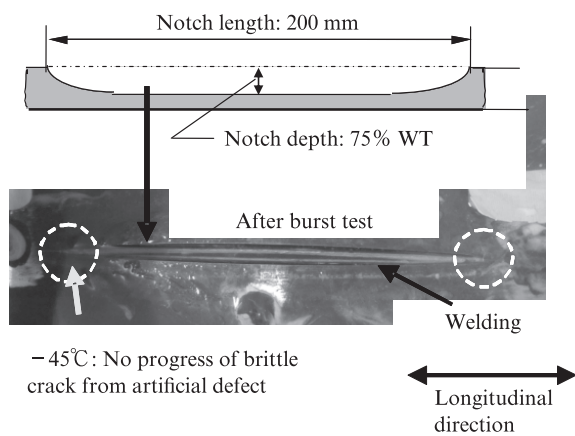


Photo 2 Low temperature full pipe burst examination result

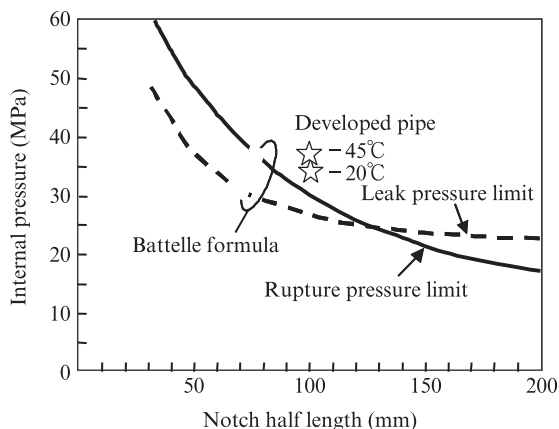


Fig. 15 Low temperature full pipe burst examination result

the Battelle prediction formula<sup>17)</sup>. This formula was developed using a considerable number of UOE hydrostatic burst test results based on UOE steel pipes, which have a long history of use. The fracture pressure of the developed pipe is higher than the estimated critical pressure. Moreover, the leak mode was ductile leaking from the bottom of the notch, demonstrating that catastrophic rupture will not occur if the pipe is used at low temperature<sup>11)</sup>. Thus, the impact on the fracture behavior of the residual stress of HFW pipes, that is stored during roll-forming seems to be small, the fracture behavior can be evaluated in the same manner as UOE pipes.

Use of the developed steel pipe enables economical and efficient construction of linepipes for gas and oil, which require high levels of safety. At present, the developed pipe is used in countries around the world, including North America, Southeast Asia, and Northern Europe, and is contributing to reducing energy costs.

#### 5. Conclusion

A high frequency electric resistance welding (HFW) technology, quality assurance technology, and quality assessment technology for HFW pipes were developed, resulting in improved mechanical properties and reliability of the HFW seam.

- (1) Visualization of HFW phenomena by direct observation clarified the fact that HFW is a melt welding process, and solidification occurs while the weld metal is pressurized.
- (2) In high frequency induction resistance welding, this research revealed that heating of the welding edge begins from the center of the work-coil, the temperature rises linearly from the work-coil exit side to the welding point, rises more sharply from just before the welding point to the welding point itself, and then decreases gradually.
- (3) Numerical analysis models were developed for the HFW welding. New knowledge was obtained, showing that increasing the welding speed is effective for reducing oxide inclusions in the weld seam.
- (4) The movement of oxide inclusions in the molten metal during pressurization was clarified by numerical analysis. Pressurization during HFW expels a

large majority of oxides which exist at the welding edge to the excess metal. Homogeneous temperature distribution in the welding edge remarkably promotes elimination of oxides.

- (5) Based on the knowledge obtained from direct observation and numerical analysis of HFW phenomena, HFW welding conditions were optimized and a homogeneous heating technology was developed. The Charpy fracture transition temperature of the developed pipe is  $-90^{\circ}\text{C}$ , and the developed pipe showed high absorbed energy in extra-low temperatures.
- (6) The results of an investigation of the HFW seam by a high sensitivity ultrasonic C-scan test with a focused probe showed that microscopic oxide inclusions with a size of several  $\mu\text{m}$  exist in a scattered distribution in the seam, and areas with a high inclusion density influence low temperature toughness.
- (7) The relationship between the echo height of the high sensitivity ultrasonic C-scan test and Charpy absorbed energy values was investigated. The results demonstrated that absorbed energy can be evaluated with high sensitivity by using an ultrasonic evaluation range of  $1\text{ mm}^2$ .
- (8) A point converging tandem beam ultrasonic inspection method was developed for detection of the distribution of microscopic oxide inclusions. In comparison with the conventional ultrasonic angled beam inspection method, sensitivity was improved by 10 times or more, making it possible to detect the distribution of oxide inclusions, which influence weld quality.
- (9) A technology for complete nondestructive inspection in the wall thickness direction and pipe axial direction of welds in HFW pipes was established. By realizing online application of this technology, it has become possible to detect and display the distribution of oxides in real time, and full-length quality assurance of the weld seam was realized.
- (10) Low temperature burst tests were conducted at  $-20^{\circ}\text{C}$  and  $-45^{\circ}\text{C}$  using full-body pipes with an arti-

ficial defect in the HFW seam. The results showed that the fracture pressure of the developed pipe is sufficiently higher than the value predicted by the Battelle prediction formula.

## References

- 1) Teikou yousetubuniokeru kekkann to tokutyou. J. W. S., Research Committee on Resistance Welding. 1987, p. 2.
- 2) Okabe, Takatoshi; Kodama, Toshifumi; Hori, Hiromichi; Toyoda, Shunsuke; Kimura, Hideto; Yasuda Koichi; Nakata Kazuhiro. Preprints of the National Meeting of J. W. S. 2013, 92, p. 223.
- 3) Okabe, Takatoshi; Yasuda, Koichi; Kodama, Toshifumi; Goto, Sota; Aratani, Masatoshi; Toyoda, Shunsuke; Kato, Yasushi; Iwazaki, Kenichi; Nakata Kazuhiro. Proc. of 66th IIW. 2013, doc. XII-2130-13.
- 4) Okabe, Takatoshi; Toyoda, Shunsuke; Kato, Yasushi; Yasuda Koichi; Nakata Kazuhiro. Preprints of the National Meeting of J. W. S. 2014, 94, p. 110.
- 5) Okabe, Takatoshi; Goto, Sota; Aratani, Masatoshi; Toyoda, Shunsuke; Kimura, Hideto; Kawanishi, Akira. Proc. of JSTP. 2013, p. 231.
- 6) Okabe, Takatoshi; Kenmochi, Kazuhito; Sakata, Kei. Tetsu-to-Hagané. 2007, vol. 93, no. 5, p. 33.
- 7) Okabe, Takatoshi; Yokoyama, Hiroyasu; Toyoda, Shunsuke; Kimura, Hideto; Kawanishi, Akira. CAMP-ISIJ. 2010, vol. 23, p. 1083.
- 8) Okabe, Takatoshi; Aratani, Masatoshi; Yokoyama, Hiroyasu; Toyoda, Shunsuke; Kimura, Hideto; Egi, Motoharu; Kawanishi, Akira. Steel Res. Int. 10th ICTP2011, p. 662.
- 9) Okabe, Takatoshi; Goto, Sota; Aratani, Masatoshi; Toyoda, Shunsuke; Kimura, Hideto; Kawanishi, Akira. CAMP-ISIJ. 2012, vol. 25, p. 391.
- 10) Inoue, Tomohiro; Suzuki, Masahito; Okabe, Takatoshi; Matui, Yutaka. JFE Technical Report. 2013, no. 18, p. 18.
- 11) Okabe, Takatoshi; Toyoda, Shunsuke; Matui Yutaka; Igi, Satoshi; Yabumoto Satoru. Materia Japan. 2014, vol. 3, no. 53, p. 104.
- 12) Iizuka, Yukinori. CAMP-ISIJ. 2011, vol. 22, p. 1052.
- 13) Iizuka, Yukinori; Yokoyama, Hiroyasu; Okabe, Takatoshi; Suzuki, Masahito; Kumazawa, Tadanobu; Inoue, Tomohiro. CAMP-ISIJ. 2011, vol. 24, p. 247.
- 14) Iizuka, Yukinori; Yokoyama, Hiroyasu; Suzuki, Masahito; Kumazawa Shintaro. JSNDI, 19th Symposium on ultrasonic testing. 2012, p. 7.
- 15) Matui, Yutaka; Iizuka, Yukinori; Urahata, Eiichi; Oka Masaru; Suzuki, Masahito. JSNDI, 19th Symposium on ultrasonic testing. 2012, p. 13.
- 16) New Engineering Review of Joining. Editorial Committee of New Engineering Review of Joining. 1994, p. 322.
- 17) Kiefner, J. F.; Maxey, W. A.; Eiber, R. J.; Duffy, A. R. ASTM STP 536, p. 461.